

*Article*

# A New Input Device for Spastics Based on Strain Gauge

Niels Buchhold \* and Christian Baumgartner \*

Institute of Health Care Engineering with European Testing and Certification Body of Medical Devices,  
Graz University of Technology, Stremayrgasse 16/II, 8010 Graz, Austria

\* Correspondence: 0603591990@t-online.de (N.B.); christian.baumgartner@tugraz.at (C.B.)

**Abstract:** This article presents a new input device for spastic patients and others with similar symptoms. The sensor consists of a disc used to determine positions and can replace standard joysticks in medical devices such as electric-powered wheelchairs. Using a standard joystick while operating a powered wheelchair can result in dangerous situations when spastic movements occur and extremities cramp making them uncontrollable. To avoid this, a disc was developed that can be controlled with any body part. By shifting weight (x- and y-axis) the disc can tilt in any direction creating a proportional output signal and can also be pushed down in the center (z-axis) to open a menu on a screen for example. When spasms occur it is impossible for users to get stuck on the input device because the disc is flat and can be mounted within a control panel. Body parts coming into contact with the disc would merely slide across the disc without triggering unintentional actions. The sensor presented here is also adaptive and can be adjusted to fit a user's strength and range of motion. This proposal aims to develop an input device that enables spastic patients to operate sensitive systems safely.

**Keywords:** tactile sensors; assistive technologies; power wheelchair; medical systems; robotic; joystick; strain-gauge; spasticity

---

## 1. Introduction

The use of sensors as interfaces between man and machine is taking on an increasingly important role in our society. Joysticks and systems similar to joysticks can be operated almost intuitively and can be found in a variety of controller systems as input devices. Fields of application such as medical technology require the highest possible level of safety. Moreover, a wide spectrum of use is necessary for individual users. For people with physical disabilities such as spasticity, using a sensor [1] (joystick) often presents a problem since the range of motion (force and lift) is prone to constant changes and unexpected spasms. Cramped movements when using sensitive systems can result in uncontrollable and dangerous situations. The user can also injure itself, for example, when a hand cramps around a joystick and the bones and tendons are overstrained [2]. When an electric-powered wheelchair is used, new control systems such as eye tracking, voice control, and brain-computer interfaces [3–6] tend to be problematic. Tongue controls [7,8] are only suitable under certain conditions. These types of input methods make it difficult to perform precise and complex control actions simultaneously. Eye tracking is also subject to natural reflexes (eye reflex) and is completely unsuitable as a control method when safety is important. Voice controls can usually only process one command at a time and are unreliable in loud environments [9]. A reliable control test with an electric-powered wheelchair (EPW) is to drive in the shape of a figure 8. Systems that provide users assistance with navigation [10,11] are practical but also costly.

Moreover, truly independent use is not possible because the navigation aid intervenes in programmed situations. Controls that observe the spastic movements over a defined period of time [12] and generate the probable directional requirement by means of an algorithm could be combined with the strain gauge disc (SGD) as the input medium. Even in this case, however, direct control

would be prevented. For sporting activities such as EPW hockey, direct controls are preferred. In US patents, [13–15] input devices with strain gauges are described that are fashioned in the form of conventional joysticks. The method of position determination used here is therefore basically known. The explicit innovations concerning known constructions and methods for position determination are listed below:

1. The sensor's specific flat disc design.
2. The construction and formation of the movement carrier made of carbon fiber reinforced composite.
3. The movement carrier's high-precision ability to return to its exact position of rest after deflection.
4. The algorithm to customize the device to changed clinical symptoms
5. The differential plausibility test of strain-gauge values to increase user safety.
6. The insensitivity of the sensor during spasticity (loadable up to 1,400 N).

All of these new features are described in this article. This includes the implementation and description of the prototypes' hardware (Figure 1 and 2) as well as the schematic description of the software and its algorithms.

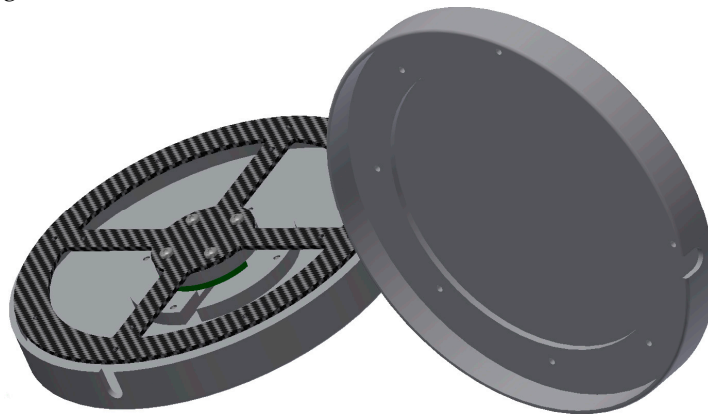


**Figure 1.** SGD drawing

## 2. Hardware of the SGD

### 2.1 Basic construction

As the sensor can be exposed to gross motor strain at times, the design is robust and can withstand loads up to 1,400 N without damage. In addition, fine motor movements need to be processed outside spasms. However, the user should at no time carry out an unwanted operation. A flat disc (120 mm diameter) appeared to be the most sensible for the reasons mentioned above. The actual sensor (see Figure 2) consists of a carbon fiber reinforced composite (CFRP) carrier (Pos. 2) to which four strain gauges are attached. Below the carrier is a circuit board (Pos. 4) with 4 differential amplifiers AD 623 [16] and an AD 7811 [17] with integrated SPI (Serial Peripheral Interface) connector. The user is thereby able to incline the disc in any direction by shifting the weight (x-, y-axis) to the upper cover (Pos. 1). The CFRP carrier is operated differentially. If a side of the CFRP carrier is pressed downwards, the opposite side of the CFRP carrier rises geometrically. This can lead to a plausibility check (see 3.2 plausibility check). The upper cover can also be operated centrally. In this case, all four strain gauges are deflected in one direction (z-axis), thus further control possibilities, such as the use of a computer mouse (mouse click), become possible. The components (items 3 and 5) of the sensor are only used as spacers. The entire sensor can also be

integrated in a control panel in front of the user (EPW operating panel). In this case, for example, the entire control table could be made of CFRP, whereby the table simultaneously represents the sensor material. Due to the interlocking housing parts, the sensor is splash-proof.

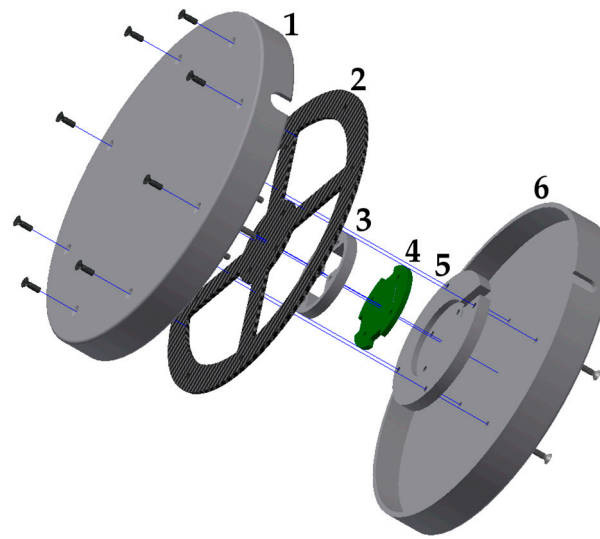
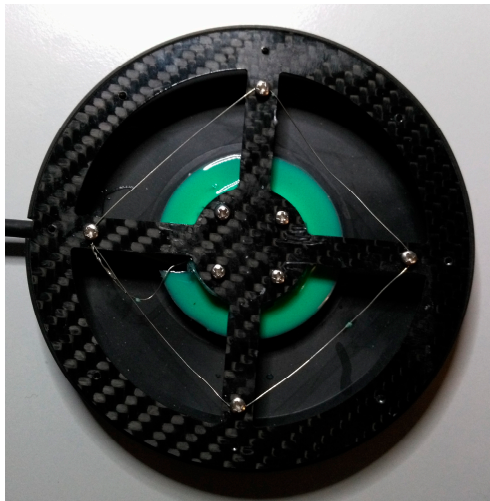


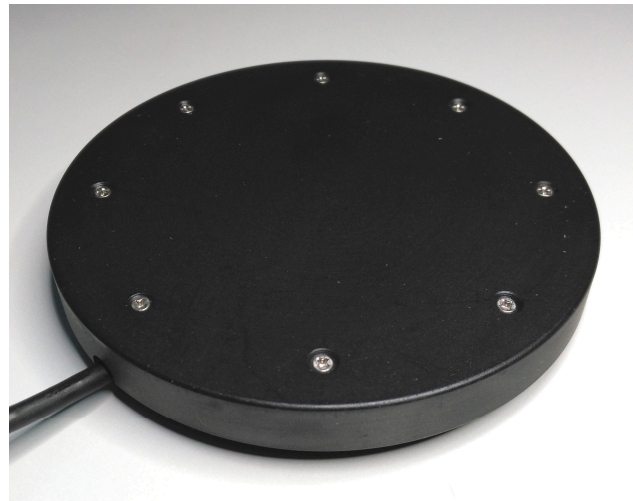
**Figure 2.** SGD exploded view drawing

The SGD consists of the following components:

1. upper case
2. CFRP carrier
3. spacer
4. circuit board
5. spacer
6. lower case



**(a)**



**(b)**

**Figure 3.** SGD without upper cover (a) and with cover (b)

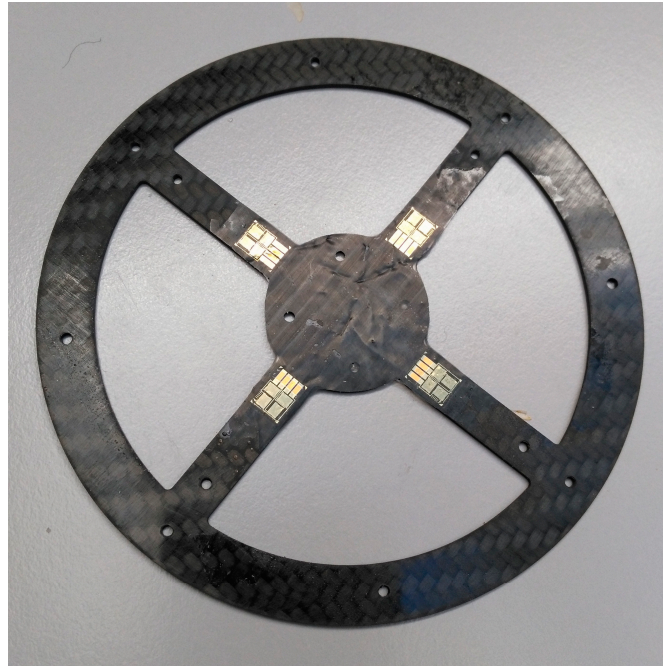


**Figure 4.** CFRP carrier with affixed strain-gauges

## 2.2 CFRP carrier

The CFRP carrier (Figure 4) of the prototype consists of a CFRP plate with a thickness of 1.3 mm. The thickness of the material can be adapted to the application, with CFRP having excellent strength as compared to other materials. Compared to aramid fiber reinforced composite (AFRP) and glass fiber reinforced composite (GFRP), CFRP has superb dynamic properties. The dynamic damping capacity of AFRP under a dynamic load six times higher than GFRP and nine times higher than CFRP [18]. In particular, the reset behavior of the CFRP carrier is important. If the sensor is overloaded, the interlocking housing parts protect the CFRP carrier against damage. Due to the design of the housing, the maximum stroke can be mechanically limited. In case of excessive stress (max. 1,400 N), inflowing forces are then discharged past the CFRP carrier over the housing. The CFRP compensated strain gauges are glued on and then soldered to the circuit board. The circuit board and the strain gauges can finally be covered with an additive-crosslinked silicone. Thus, the sensor can also be used in a humid environment. The CFRP carrier was also tested for tension. The construction shown in Figure 3 with a material thickness of 1.3 mm broke under a tensile load of 102 N. It is impossible, however, to overload the sensor housing in that way without the aid of a tool. The chosen material thickness of 1.3 mm provides a very good compromise between sensitivity and durability.

## 2.3 Circuit board

Four differential amplifiers (Fig. 2, Pos. 4), a 10 bit A/D converter and voltage stabilization are on the circuit board. The amplification of the differential amplifiers is set with an external resistor. All four analog values are continuously queried via the 4-channel ADC (analog digital converter) and passed on to a downstream microcontroller via an SPI interface.

## 2.4 Different versions

Depending on the purpose of use, the sensor can be operated in different variations:

Version 1: The CFRP carrier and its shape are adapted to the expected requirements. In particular, the material thickness and the arrangement of the CFRP fabric coverings are taken into account. The shape also supports the stability and varies the bending stress of the strain gauges.

Version 2: The setup is similar to version 1. In addition, the CFRP carrier is poured into an additive-crosslinked, thermally vulcanizing silicone rubber. Depending on the Shore hardness, the damping properties are thereby varied. Other damping materials, such as compression springs or other polymers, did not bring about the desired effect because the thermal expansion coefficients influenced the CFRP carrier in a counterproductive manner.

Version 3: The entire operating panel (e.g. on an EPW) is made of CFRP. The strain gauges are applied underneath the panel. Milling patterns around the strain gauges then vary the input forces applied by the user.

During the series of tests, CFRP carriers with material thicknesses from 0.45 mm to 2 mm were examined. The shape can also influence and adjust the sensitivity and maximum load and in particular the force required.

## 3. Sensor operations

### 3.1 Basics

If external forces act on the CFRP carrier over the upper side of the housing, the angle will change slightly. As a result, the opposing strain gauge is deflected differentially. The resulting differential values can be added to the downstream microcontroller in order to increase the technical resolution. If, for example, a 10 bit A / D converter is used, the resolution increases accordingly.

Example Calculation:

$X_{Neutral} = 512 \text{ digits};$	Measured neutral value;
$X_{Right\ t=1} = 640 \text{ digits};$	Measured value right strain gauges at $t = 1$ ;
$X_{Left\ t=1} = 430 \text{ digits};$	Measured value left strain gauges at $t = 1$ ;
$X_{t=1} =  X_{Neutral} - X_{Right\ t=1}  +  X_{Neutral} - X_{Left\ t=1} $	
$X_{t=1} = 210 \text{ digits}$	Output x-value to the microcontroller

Depending on the version used, the restoring force of the moving support is via the CFRP alone or additionally via a silicone rubber. In Table 1 and Fig. 5, the digits achieved are shown in relation to the force acting. Various silicone rubber mixtures and material strengths are shown here as examples. Due to the fact that the measurement curves are identical in each direction and for each strain gauge, the measurement was carried out for just one strain gauge. In addition to the maximum 1024 digits, additional forces flow over the housing.



**Table 1.** Selected measurements with different materials and versions. (only  $X_{Right}$  is shown)

Test series force												
(N)/digits	0	0.05	0.1	0.2	0.5	1	2	3	5	10	20	25
diameter disc 110 mm												
1 Mat. CFRP 0.45 mm												
non silicon rubber	532	538	545	561	592	650	760	890	1024	1024	1024	1024
2 Mat. CFRP 0.90 mm												
non silicon rubber	535	537	540	551	569	622	698	810	903	1024	1024	1024
3 Mat. CFRP 1.30 mm												
non silicon rubber	510	511	513	516	529	550	611	675	776	895	1024	1024
4 Mat. CFRP 2.00 mm												
non silicon rubber	521	521	521	521	522	528	549	607	673	790	897	1024
5 Mat. CFRP 0.90 mm												
silicon rubber shore 20	505	506	507	511	558	611	670	796	881	982	1024	1024
6 Mat. CFRP 0.45 mm												
silicon rubber shore 30	535	537	542	561	614	666	791	873	970	1024	1024	1024

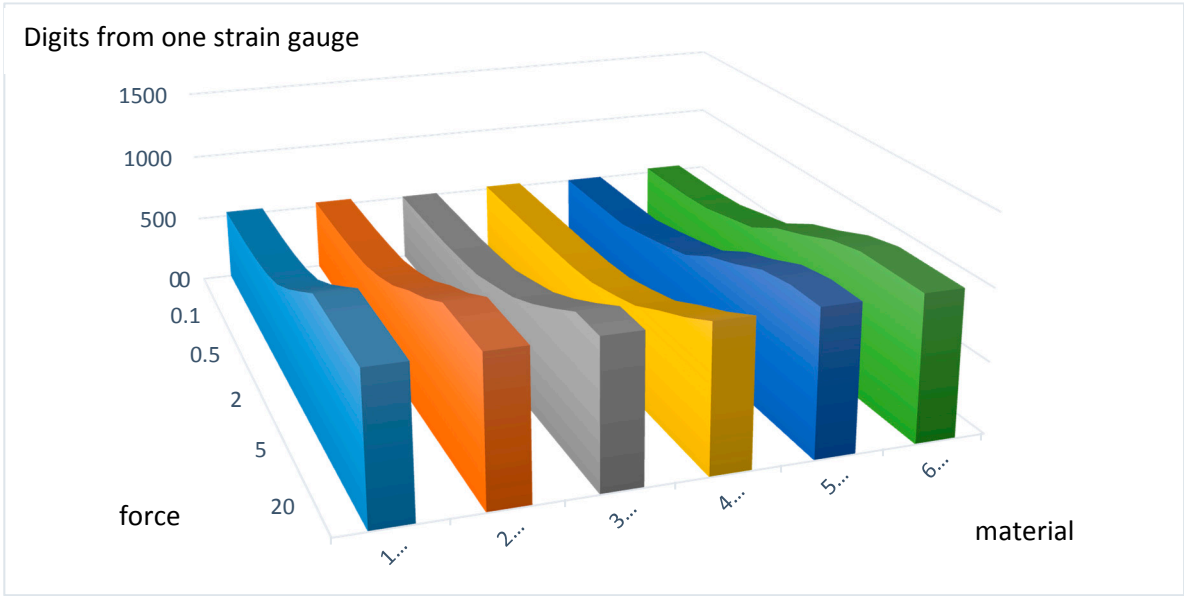


**Figure 5.** Visualized, measured values from table 1

3.2 Plausibility check

The sensor will also be utilized in highly sensitive or safety related areas, therefore a plausibility check is necessary. For this purpose, in an individual calibration process, all possible measured value combinations of the individual strain gauges are stored in a hash table. If a strain gauge is released from the CFRP carrier, a specific measured value is recorded. In the hash table, a stored value of the opposite, differentially working strain gauge is searched for this measured value. If this value pair does not match the currently measured value pair, then there must be an error. Direct measures are then taken to protect the downstream system from malfunctions.

3.4 Individually adjustment of the strain gauge disk

Due to the various symptoms of individual medical conditions, different input forces and input lifts are required. Depending on the specifications, standard joysticks have a pre-determined accuracy (resolution), a certain amount of force is required to deflect it, and a certain stroke to overcome the necessary paths by a fixed amount. As described in the introduction, certain groups of physically disabled people are unable to use standardized joysticks. The issue has to do with this group of individuals' range of motion in terms of force and stroke. Moreover, the existing range of motion is affected by outside influences such as the ambient temperature [19]. A permanent readjustment of the sensor would be necessary for long-term use. To adjust the sensor to the user's movement and stroke characteristics, the user moves the SGD at least once with a circular movement in each direction. The z-axis can also be configured by using vertical pressure on the housing cover. The maxima of the x-, y-, and z-coordinates are then saved. The absolute zero position or resting position of each SGD is set during calibration. The calibration process usually takes place only once after production. This avoids higher production costs since the manufacturing allowances are relatively insignificant. As an example, the force or the stroke of a patient was documented. The result in Figure 6 shows an inhomogeneous progression of force applied in different directions.

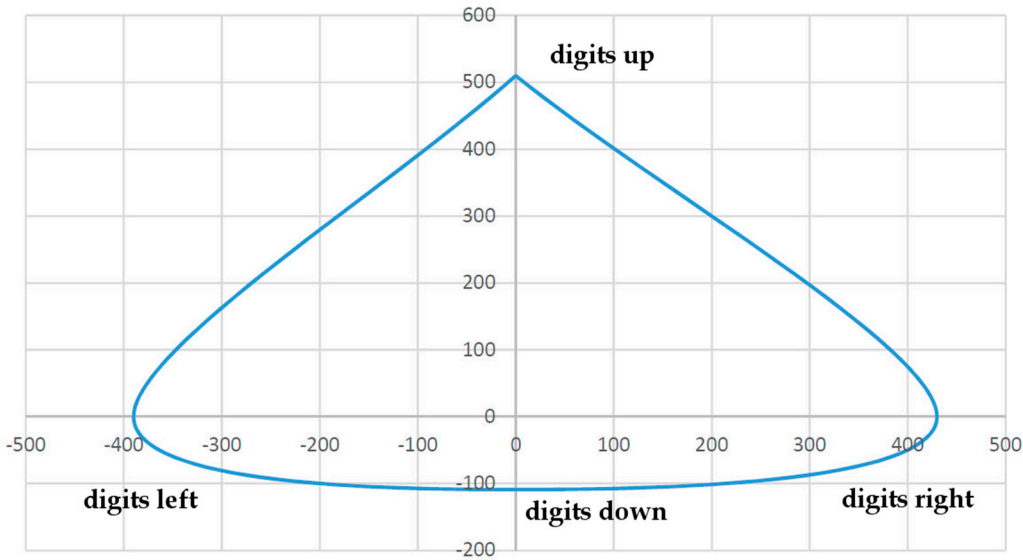


Figure 6. Force Curve (force to digit), max. value from neutral position Material 3 (see table 2)

When a reference was established (deflection and force to digit) Figure 6 can be used to directly determine the force and stroke the patient applied (see table 2. In a test case, the patient was able to carry out the following deflections, i.e. force (the z-axis is not taken into account here):

Table 2. Patient measurements and applied force.

Direction To	Maximum Digits	Approximate Force
forward	510	18.4 N
back	109	2.1 N
left	390	11 N
right	430	14.2 N

These values cannot be transmitted directly to an EPW. The patient would be able to drive the wheelchair forward, to the right and to the left. The values achieved for backwards are not sufficient, however, to move the wheelchair. Suitable factors can provide the desired consistent output signal.

Example: Common output values are in the 10 bit range (1024 / value = factor).

**Table 3.** Maximum patient measurements and calculated output values.

Direction To	Maximum Digits	Factor	Calculated Output Values
forward	510	2,007	1024
back	109	9,394	1024
left	390	2,626	1024
right	430	2,381	1024

All of the coordinates documented during use for this user, then have to be converted with the factor to attain a consistent output signal.

Example Calculation:

(Right value see Table 2; 10 bit output signal)

$X_{MaxRight} = 430 \text{ digits};$

Maximum right direction;

$X_{FactorRight} 2,381$

Calculated factor see table 3;

$X_{RightExample} = 200 \text{ digits};$

Example value to the right;

$X_{OutRight} = X_{RightExample} * X_{FactorRight}$

Digital output value;

$X_{OutRight} = 476 \text{ digits}$

Digital output;

These initial values are then calculated with the differential output value of the opposite strain gauge, according to the example calculation (see 3.1 Basics). During this time, the plausibility check (see 3.2 Plausibility check) is also performed. By means of the algorithm shown above, the coordinates of the inhomogeneous input forces (see Figure 6) are converted into homogeneous output data (see Figure 7). The user can then, for example, move a computer mouse or an EPW at the same speed in all directions independently of its inhomogeneous force-lifting ratio. The output values calculated by the factor are denoted in Table 3 and visualized in Figure 7.

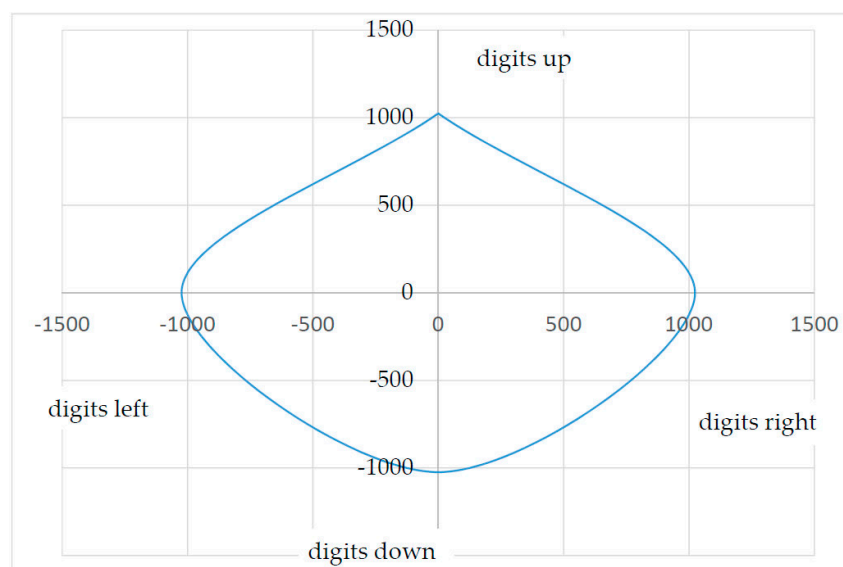


**Figure 7.** Output data curve.



### 3.5. Software

The software sequences are divided into two separate processes. To adapt the SGD to the user (see Figure 8), the teach-in-button must be pressed. After the rest values have been determined, the microcontroller stores the maximum values reached for each individual direction. In addition, possible value combinations are stored, which are then used for plausibility checks. After determining all the values mentioned, factors are calculated in order to generate homogeneous output signals (see Figure 7) from the inhomogeneous input signals (see Figure 6). If the rest values are outside a defined range (theoretical rest value  $\pm 100$  digits), an error is generated. This value range serves to balance manufacturing tolerances.

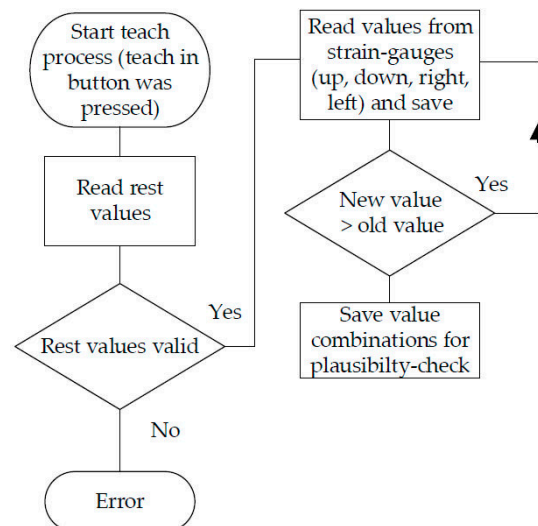


**Figure 8.** Schematic sensor software teach-in process.

During normal use (see Figure 9), the data of the AD 7811 are first read in via SPI. Then, a plausibility check is performed. In this case, two strain gauges are combined as a pair of values. These pairs of values must match the value pairs stored in the teach-in-process. Thus, a very large portion of all possible errors can be intercepted. In case of an error, the microcontroller sends neutral values to the connected systems and a separate error message is issued via an I/O pin.

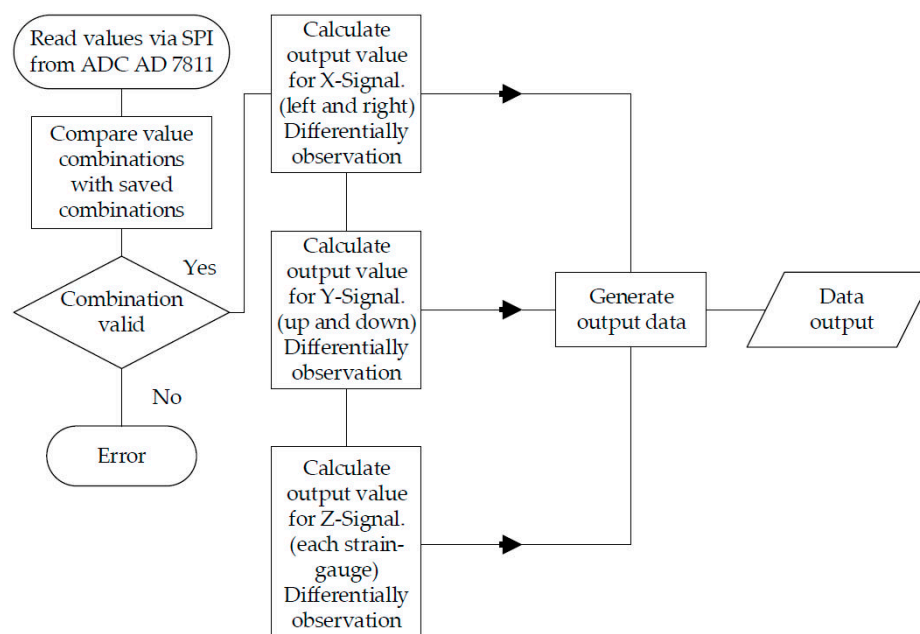


**Figure 9.** Schematic sensor software under normal use.

### 3.6. Hardware

The measured output signals (Fig. 10) of the 4 strain gauges are amplified with the respective differential amplifier AD 623 [16]. The analog voltage values are then fed in with an ADC (analogue digital converter) AD 7811[17] and converted into an SPI (slave) bus signal. A microcontroller SPI (master) accepts the data and generates the desired output signals for the connected hardware. The microcontroller also utilizes various input and output signals, which in the event that the SGD malfunctions an emergency signal is sent to an EPW.

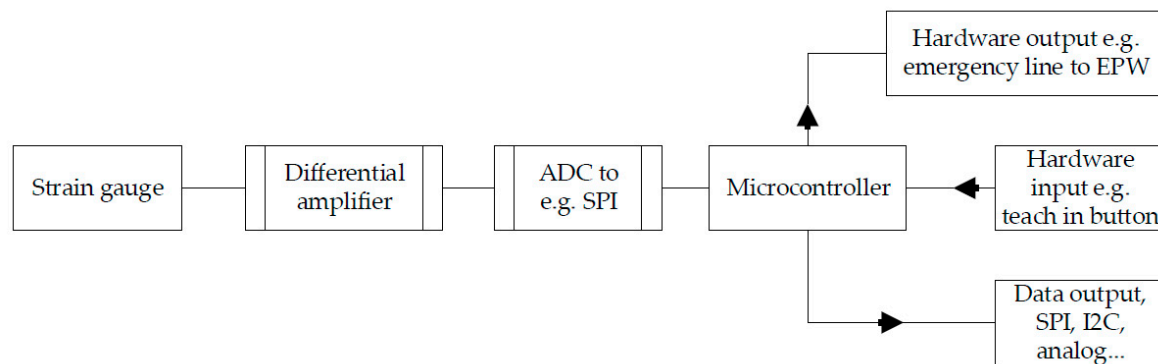


**Figure 10.** Schematic sensor hardware.

## 4. Results and Discussion

The SGD described here is in the prototype stage. Using CFRP the spring precision is at  $\pm 1$  digit. The climate chamber tests were successfully completed ( $-30$  degrees to  $80$  degrees) with a deviation of  $\pm 1$  digit. This can lead to a maximum  $\pm 2$  digits deviation due to external influences. To counteract this problem, a rest window of 5 digits is set in each direction around the neutral parent values. The first tests under laboratory conditions were successfully completed. During the tests, the sensor was used to substitute a mouse and to operate an EPW [20]. As long as a physically disabled patient still has some type of physical capability (hand, finger, foot, head, shoulder, etc.), use of this SGD should be possible. If the disease pattern changes, the SGD can be adapted immediately (without specialist staff) to the user's new abilities. This learning process takes a maximum of 10 seconds. Especially in countries with poor health systems, using the SGD is beneficial because practically no follow-up costs are to be expected even if the SGD is used by another user with a different medical condition. Due to the weight of the upper housing cover, the SGD can begin to oscillate when a specific frequency acts on the sensor. Thus the system can begin to "vibrate". This particular case can also occur in off-the-shelf joysticks. In order to prevent this unlikely event, an additive-cross-linked silicone rubber can be poured under the CFRP carrier (version 2), which acts as a vibration damper, alleviating the vibration. Due to the design, the force to be exerted increases exponentially to the deflection, thereby causing a natural force feedback.

In summary, this sensor provides a new input possibility, especially for spastic patients. Injuries or an unintentional invoke of commands due to sudden spasticity are largely avoided. Combined with other recent developments as cited in the introduction, the human-machine interface could be improved for this disease. Due to the simple construction of the SGD, high production costs are not expected. Testing according to the Medical Devices Act has not yet been carried out.

**Author Contributions:** The contributions of this paper are related to the PhD thesis of Niels Buchhold (conception, prototype design, paper writing). Christian Baumgartner is his thesis supervisor (conception, paper writing).

**Conflicts of Interest:** The authors declare no conflicts of interest.

## References and Notes

1. Buchhold, N.; Baumgartner, C. A New, Adaptable, Optical High-Resolution 3-Axis Sensor. *Sensors (Basel, Switzerland)* **2017**, *17*.
2. Hu, X.; Afsharipour, B.; Rymer, W.Z.; Suresh, N.L. Impairment of muscle force transmission in spastic-paretic muscles of stroke survivors. In *2016 38th annual international conference of the IEEE Engineering in Medicine and Biology Society (EMBC)*; IEEE: Piscataway, NJ, 2016, pp. 6098–6101.
3. Wolpaw, J.R.; Birbaumer, N.; Heetderks, W.J.; McFarland, D.J.; Peckham, P.H.; Schalk, G.; Donchin, E.; Quatrano, L.A.; Robinson, C.J.; Vaughan, T.M. Brain-computer interface technology: a review of the first international meeting. *IEEE transactions on rehabilitation engineering : a publication of the IEEE Engineering in Medicine and Biology Society* **2000**, *8*, 164–173.
4. Kim, K.-N.; Ramakrishna, R.S. Vision-based eye-gaze tracking for human computer interface. In *IEEE SMC'99 conference proceedings*; IEEE Service Center: Piscataway, NJ, 1999, pp. 324–329.
5. Malkin, J.; House, B.; Bilmes, J. Control of simulated arm with the vocal joystick. CHI 2007 Workshop on Striking a C [h] ord: Vocal Interaction in Assistive Technologies, Games, and More. *CHI 2007 Workshop on Striking a C [h] ord: Vocal Interaction in Assistive Technologies, Games, and More* **2007**.
6. Malkin, J.; House, B.; Bilmes, J. The VoiceBot: a voice controlled robot arm. Vocal Interaction in Assistive Technologies, Games, and More. *CHI 2007 Workshop on Striking a C [h] ord* **2007**, 183–192.
7. Buchhold, N. *Apparatus for controlling peripheral devices through tongue movement, and method of processing control signals*. US Patent 5460186 A, 24. Okt. 1995.
8. Kim, J.; Park, H.; Ghovanloo, M. Tongue-operated assistive technology with access to common smartphone applications via Bluetooth link. *Conference proceedings : ... Annual International Conference of the IEEE Engineering in Medicine and Biology Society. IEEE Engineering in Medicine and Biology Society. Annual Conference* **2012**, 2012, 4054–4057.
9. Martens, C.; Ruchel, N.; Lang, O.; Ivlev, O.; Graser, A. A friend for assisting handicapped people. *IEEE Robotics & Automation Magazine* **2001**, *8*, 57–65.
10. Huntemann, A.; Demeester, E.; Poorten, E.V.; van Brussel, H.; Schutter, J. de. Probabilistic approach to recognize local navigation plans by fusing past driving information with a personalized user model. In *IEEE International Conference on Robotics and Automation (ICRA)*, 2013, 6 - 10 May 2013, Karlsruhe, Germany; IEEE: Piscataway, NJ, 2013, pp. 4376–4383.
11. Kim, E.Y. Wheelchair navigation system for disabled and elderly people. *Sensors* **2016**, *16*, 1806.
12. Cooper, R.A.; Widman, L.M.; Jones, D.K.; Robertson, R.N.; Ster, J.F. Force sensing control for electric powered wheelchairs. *IEEE Transactions on Control Systems Technology* **2000**, *8*, 112–117.
13. Kamentser, B.; Kamentser, E. *Force transducer with co-planar strain gauges*. U.S. Patent No. 5,872,320, 16. Febr. 1999.
14. Manara, A.; Scofield, M.C.; Cheal, B. *Sensor and circuit architecture for three axis strain gauge pointing device and force transducer*. U.S. Patent No. 6,243,077, 5. June 2001.
15. Nejedly, P.; Whitfield, D.W. *Three dimensional strain gage transducer*. U.S. Patent No. 4,217,569., 12. Aug. 1980.

16. Analog Devices Inc. *AD623 (Rev. E)*. Available online: <http://www.analog.com/media/en/technical-documentation/data-sheets/AD623.pdf> (accessed on 1 January, 2017).
17. Analog Devices Inc. *AD7811/AD7812 (Rev. C)*. Available online: [http://www.analog.com/media/en/technical-documentation/data-sheets/AD7811\\_7812.pdf](http://www.analog.com/media/en/technical-documentation/data-sheets/AD7811_7812.pdf) (accessed on 1 January, 2017).
18. Ehrenstein, G.W. *Faserverbund-Kunststoffe: Werkstoffe, Verarbeitung, Eigenschaften*, 2nd ed; Hanser Verlag: München, 2006.
19. Muscular Dystrophy Association Inc. *Facts About Myotonic Muscular Dystrophy*. Available online: [https://www.mda.org/sites/default/files/publications/Facts\\_MMD\\_P-212\\_0.pdf](https://www.mda.org/sites/default/files/publications/Facts_MMD_P-212_0.pdf) (accessed on 1 January, 2017).
20. Dynamic Controls. *The DX2 System - Dynamic Controls*. Available online: <https://dynamiccontrols.com/en/dealers/products/dx2/the-dx2-system> (accessed on 1 January, 2017).
21. Thorp, E.B.; Abdollahi, F.; Chen, D.; Farshchiansadegh, A.; Lee, M.-H.; Pedersen, J.P.; Pierella, C.; Roth, E.J.; Seanez Gonzalez, I.; Mussa-Ivaldi, F.A. Upper Body-Based Power Wheelchair Control Interface for Individuals With Tetraplegia. *IEEE transactions on neural systems and rehabilitation engineering : a publication of the IEEE Engineering in Medicine and Biology Society* **2016**, *24*, 249–260.



© 2017 by the authors; licensee *Preprints*, Basel, Switzerland. This article is an open access article distributed under the terms and conditions of the Creative Commons by Attribution (CC-BY) license (<http://creativecommons.org/licenses/by/4.0/>).